

RESEARCH

Open Access



Smart sustainable concrete: enhancing the strength and durability with nano silica

Vikram Singh Kashyap¹, Gaurav Sancheti¹, Jitendra Singh Yadav^{2*} and Utkarsh Agrawal¹

Abstract

A detailed investigation was conducted to analyse the mechanical and durability features of a mixture of binary cement concrete modified with nanomaterials. In the context of the concrete matrix, the substitution of fractional cement content was carried out using Nano silica (NS) at concentrations of 1%, 2%, and 3%. Four distinct cementitious blends were subjected to a comprehensive match of tests, which encompassed compressive strength, flexural strength, split tensile strength, static modulus of elasticity, bulk density, water absorption, permeability, carbonation resistance, acid attack resistance, and rapid chloride penetration. The compositions of the mixes were investigated through the use of various microstructural analysis techniques, including scanning electron microscopy (SEM), energy-dispersive X-ray spectroscopy (SEM-EDS), thermogravimetric analysis (TGA), X-ray diffraction (XRD), and Fourier-transform infrared spectroscopy (FTIR). The research revealed significant improvements in the mechanical and durability characteristics of the material. An increment in the mechanical and durability properties of mixtures were seen due to inclusion of marble powder and Nano silica due to enhanced pozzolanic activities of composite and its filling effect. It is worth mentioning that Nano silica has shown the potential to mitigate the degradation caused by exposure to sulfuric acid. The SEM-EDX analysis demonstrated a decrease in the Ca/Si ratio when compared to the reference combination, suggesting an increase in the consumption of calcium hydroxide (CH) and the creation of a more compact calcium-silicate-hydrate (C-S-H) gel. The X-ray diffraction (XRD) findings indicate that NS has the ability to act as an accelerator for pozzolanic processes. This is achieved by consuming calcium hydroxide (CH) and promoting the creation of extra calcium silicate hydrate (C-S-H), which ultimately enhances the overall performance of the concrete mixture.

Keywords Cement concrete, Nano silica, Mechanical and durability performance

1 Introduction

In the modern construction landscape, ordinary Portland cement (OPC) has long been the material of choice for constructing buildings and other public structures. However, the rapid pace of urbanization has led to a significant increase in concrete production, raising concerns about its implications for climate change, resource

depletion, and environmental degradation. Cement manufacturing, a critical component of concrete production, contributes to carbon dioxide emissions, air and water pollution, and the depletion of raw materials [1]. Notably, the production of one ton of cement releases one ton of carbon dioxide and consumes approximately 1.7 tons of raw materials. While concrete is formed by combining water, binder, and particles, unreacted cement grains post-hydration remains ineffective contributors to material strength, resulting in challenges related to sustainability and cost-effectiveness [2, 3].

To address these challenges, the concept of substituting unreacted cement particles with alternative materials with similar particle size distribution and reactivity has

*Correspondence:

Jitendra Singh Yadav
jsyadav@nitkkr.ac.in

¹ Department of Civil Engineering, Manipal University Jaipur, Jaipur, India

² Department of Civil Engineering, National Institute of Technology Kurukshetra, Kurukshetra, India

gained traction. The reactivity of such supplementary cementitious materials (SCMs) is influenced by factors such as alumina concentration, excess calcium hydroxide (CH), specific surface area, and particle size. The pozzolanic reaction of SCMs upon hydration leads to the formation of a secondary C-S-H gel [4, 5]. Notably, Nano silica, owing to its remarkably small particle size, holds the potential to infiltrate the microstructure of cementitious systems and enhance the density of the concrete matrix [6]. Previous studies have indicated that incorporating Nano silica can yield significant enhancements in the mechanical properties of concrete. For instance, research by Li et al. [7] demonstrated a 24% increase in flexural strength with the inclusion of 3% and 5% Nano silica. Similarly, Zhang et al. [8] observed a 30% and 25% boost in compressive strength after 3 and 7 days, respectively, with the addition of 2% Nano silica. This trend was further affirmed by Palla et al. [9], who reported a 23% increase in flexural strength through the incorporation of 2% Nano silica.

Beyond strength improvements, Nano silica's extensive specific surface area necessitates careful consideration of its impact on the concrete mixture's rheological properties, requiring an elevated dosage of superplasticizer for proper workability [10]. Furthermore, the intrusion of potentially damaging chemicals into concrete through microporous pores and capillaries can be mitigated using Nano silica and mineral admixtures, both of which can bolster the composition's resilience [11, 12]. Notably, Nano silica's pozzolanic properties lead to the formation of finely hydrated phases like C-S-H gel, contributing to the densification of microstructure and the enhancement of mechanical characteristics. Comparative studies have even revealed Nano silica's accelerated hydration and strengthening effects, surpassing those of silica fumes [13, 14].

The positive implications of Nano silica extend to various facets of concrete performance. Its capacity to enhance the connection between cement matrix and aggregate, reduce water permeability and porosity, and improve durability has been demonstrated through multiple investigations [15, 16]. Studies by Fallah and Nematzadeh [17] showcase the ability of Nano silica to reduce the porosity of concrete, thereby lowering water absorption and enhancing the material's durability. Additionally, Nano silica's ability to absorb calcium hydroxide from cement hydration, as evidenced by Cheng [18], fortifies the cement-aggregate interface and boosts durability. Furthermore, Shaban et al. [19] Nano silica has been found to enhance concrete's resistance to acid rain and mitigate the effects of long-term sulfate attack [20, 21].

Given the compelling insights from prior research, the present study aims to delve deeper into the mechanical,

durability, and microstructural impacts of incorporating Nano silica at varying weight percentages within concrete mixtures. By exploring these effects, this research strives to contribute to the advancement of smart and sustainable construction practices, aligning with the principles of modern urban development.

The outcomes of this study bear significant implications for both the practical construction industry and the broader context of smart and sustainable urban development. The investigation into the mechanical and durability characteristics of concrete mixtures enriched with Nano silica has not only advanced our understanding of material behavior but also laid the groundwork for more sustainable and intelligent construction practices.

The integration of Nano silica has demonstrated a substantial positive impact on the mechanical properties of concrete. The increase in flexural and compressive strengths observed across various studies [7–9] is a promising development that holds the potential to lead to more robust and resilient structures. This is particularly significant for urban environments, where buildings and infrastructure are subjected to varying loads, stresses, and environmental conditions. Enhanced mechanical strength translates to longer service life, reduced maintenance requirements, and ultimately lower life-cycle costs.

Furthermore, the improved durability properties of concrete modified with Nano silica offer a multifaceted advantage for urban construction. Concrete is often exposed to aggressive external factors such as carbonation, acid attack, and chloride penetration, which can compromise its integrity over time. The ability of Nano silica to enhance resistance against these deterioration mechanisms can significantly extend the lifespan of concrete structures, mitigating the need for premature replacements and reducing resource consumption. This is a pivotal aspect of sustainable construction, aligning with the goals of minimizing waste and optimizing resource utilization.

The concept of smart cities revolves around harnessing technological advancements to optimize urban living, resource management, and environmental sustainability. In this context, the integration of smart materials, like Nano silica-modified concrete, is a notable stride towards realizing the vision of smart cities. The enhanced properties of such materials contribute to the construction of resilient infrastructure that can withstand the challenges posed by rapid urbanization, climate change, and increased energy demands.

Nano silica-modified concrete exemplifies a smart material due to its dynamic response to external stimuli and its capacity to adapt to changing conditions. The microstructural improvements resulting from Nano silica's presence align with the idea of self-healing

materials, where the material’s inherent properties enable it to repair small cracks and fissures over time. This self-healing capability contributes to the longevity of structures and reduces the need for frequent interventions, fostering a more sustainable approach to infrastructure management.

Moreover, the reduced permeability of Nano silica-modified concrete offers a direct advantage for smart cities’ infrastructure. Concrete with enhanced impermeability is less susceptible to moisture ingress, reducing the likelihood of corrosion in reinforcement steel. Corrosion-related damages are a significant concern for urban structures, and the implementation of materials that mitigate this issue is in line with the sustainability goals of minimizing maintenance needs and extending infrastructure lifespans.

2 Materials and methodology

2.1 Materials

In this study, Nano-silica (NS) was employed as a partial substitute for cement, with varying concentrations of 1%, 2%, and 3%. The Nano-silica had an average particle size ranging from 20 to 30 nm. The NS powder, characterised by a density of 2.5 g/cm³ and a specific surface area of 600 m²/g, displayed a discernible foggy aggregation pattern, as illustrated in Fig. 1. The X-ray diffraction (XRD) pattern of the NS sample, as shown in Fig. 2, exhibited a distinct peak in the angular range of 15° to 31°, suggesting the amorphous nature of the material. The trials utilised

commercially available 43-grade ordinary Portland cement (OPC) that conformed to the criteria outlined in IS 8112:1989 [22]. Table 1 provides a comprehensive overview of the physical properties that align with the standards given in the OPC IS code. Furthermore, Figs. 2 and 3 depict the X-ray diffraction (XRD) and scanning electron microscopy (SEM) spectra of the ordinary Portland cement (OPC) utilised in the investigation.

2.2 Mix proportion

In this experiment, four concrete mixtures that comply with IS 10262:2009 are listed in Table 2. IS steel moulds cast concrete samples. At 27 °C, samples of concrete were covered with plastic and held in the moulds for 24 h. Samples that were deformed were treated in portable water. In addition to morphology and mineralogy, the effects of NS (1%, 2%, and 3%) were investigated on the compressive strength, flexural strength, splitting tensile strength, and static modulus of elasticity of concrete after 1, 3, 7, 14, 28, 56, and 90 days of curing. This research used a water-to-cement ratio of 0.40.

2.3 Test conducted

2.3.1 Compressive strength

In this work, the increase of compressive strength and its sensitivity to the addition of NS were evaluated in order to quantify strength gain. Unlike the control mix, the results demonstrate compressive strength variation with NS changes (CM). IS 516-1959 tested concrete samples

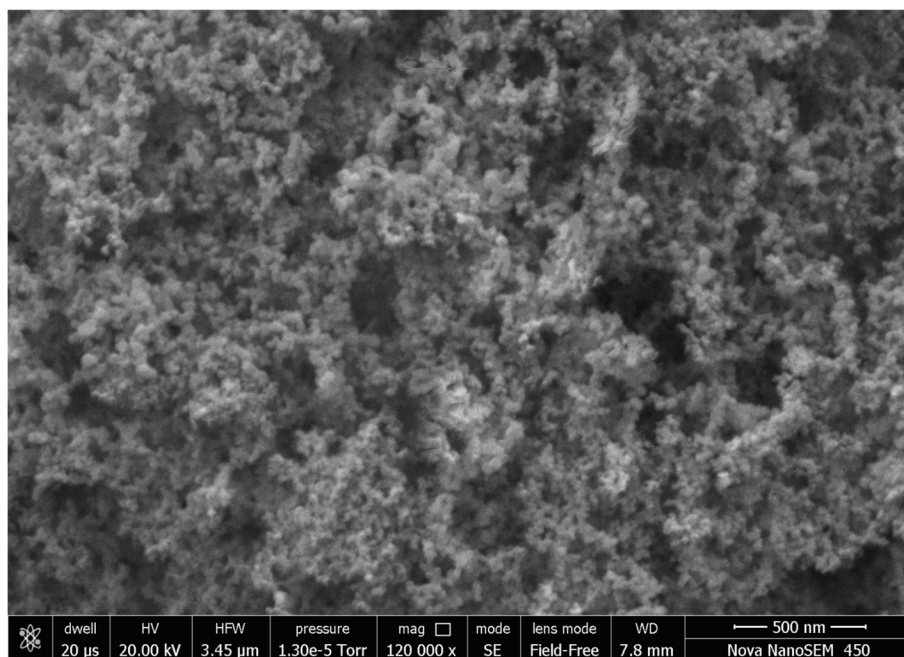


Fig. 1 SEM image of Nano silica

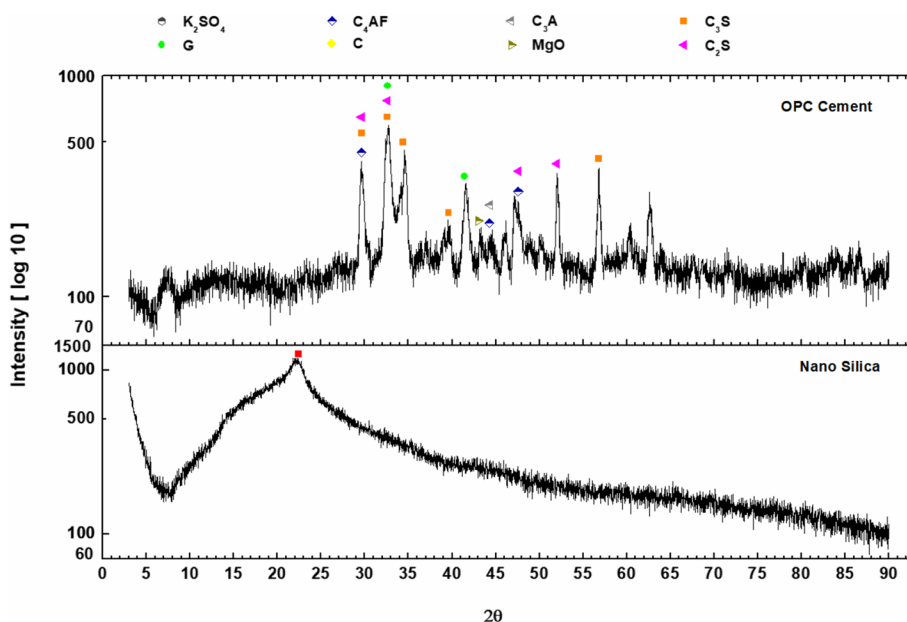


Fig. 2 XRD spectrum of OPC cement and Nano silica

Table 1 Properties of OPC

Properties	Test values
Specific gravity	3.11
Consistency (%)	32
Initial setting time (min)	60
Final setting time (min)	270
Soundness (mm)	1.5
Mortar compressive strength (Mpa)	
3 days	26
7 days	37
28 days	48

measuring 100 mm x 100 mm x 100 mm at 140 kg/sq. cm/min to determine compressive strength after the requisite number of hydration days.

2.3.2 Flexural strength

The flexural test was conducted in accordance with IS 516-1959 [23] with four-point loading at 180 kg/min on a simple beam with samples of 100 mm x 100 mm x 500 mm prismatic beams after 3, 7, 28, 56, and 90 days of water cure.

2.3.3 Split tensile strength

According to IS: 5816-1999 [24], split tensile strength (STS) tests were conducted at 1.2 N/(mm²/min). This study created cylinder-shaped concrete samples with

dimensions of 300 mm in height and 150 mm in diameter from four distinct concrete mixtures and evaluated their split tensile strength after 3, 7, 28, and 90 days of curing. The split tensile strength was determined by averaging the results of three STS tests conducted on samples.

2.3.4 Static modulus of elasticity

The static modulus of elasticity (SMOE) of concrete is a design parameter that governs the deformation of structural components. To reduce deformation and swaying, bridges and massive structures are constructed using high-modulus concrete. ASTM C469-02 [25] set the modulus of elasticity, and 150 mm x 300 mm cylinders were used to determine the SOME for each concrete mixture.

2.3.5 Bulk density test

IS:6441(Part-1) [26] calculated the bulk density of all concrete specimens based on the mass per unit volume of 100 mm cube-shaped examples. To achieve consistent weight, specimens were oven-dried for 24 h at 100 degrees Celsius. They were weighed upon cooling to room temperature.

2.3.6 Water absorption test

The water absorption test was conducted in accordance with ASTM C642-06 [27]. The 150 mm cubes of oven-dried concrete were submerged in water for 24 h. The initial and ultimate weights of the specimens were

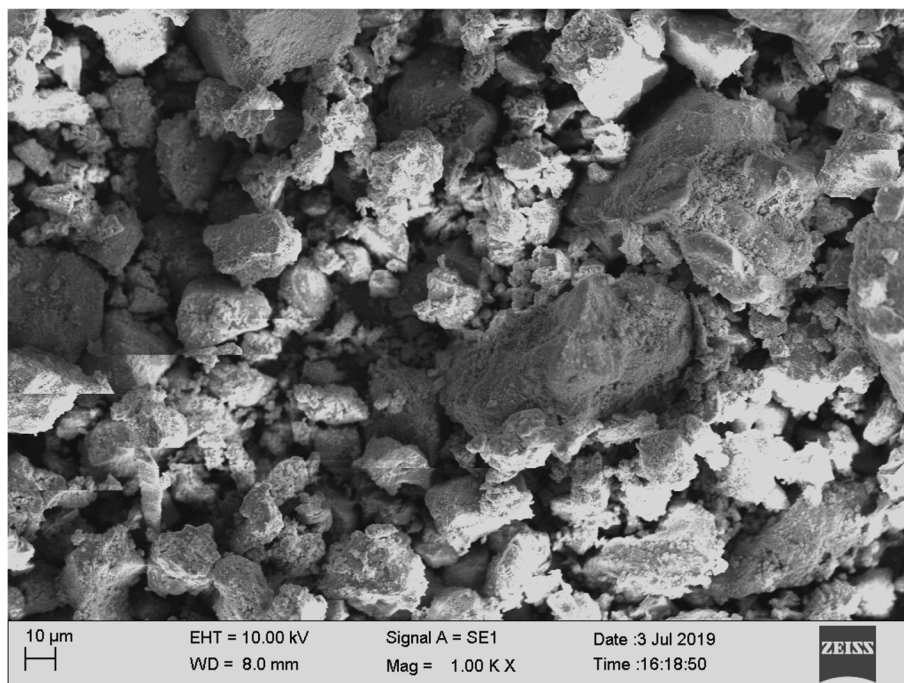


Fig. 3 SEM image of OPC cement

Table 2 Mix proportion

Mix ID	Mix Series	Notes	Binder (kg/m ³)		Fine aggregates (kg/m ³)	Coarse aggregates (kg/m ³)
			Cement	Nano Silica		
C100	NS0-C100	Control Mix	395	0	676.3	1204.6
C99	NS1-C99	Nano Silica replacement	371.3	3.95	676.3	1204.6
C98	NS2-C98		351.55	3.95	676.3	1204.6
C97	NS3-C97		331.8	3.95	676.3	1204.6

recorded, and water absorption was computed using established test procedures.

2.3.7 Din permeability test

Pore size, distribution, and microstructure influence the water permeability of concrete mixtures. Indirectly, the volumetric fraction of voids that contribute to permeability assesses the porosity of concrete. Diverse compositions of water-cured concrete specimens were examined for water permeability in accordance with DIN 1048 (Part-5) [28]. 150 mm cube specimen's oven-dried for 3 days at 55 degrees Celsius. The specimens were evaluated for 3 days at 0.5 N/mm² pressure. On a compressive testing machine, all specimens of various compositions were split in half to assess water penetration.

2.3.8 Carbonation test

Using CPC-18 and RILEM standard procedures, the carbonation of concrete mixtures was evaluated. At 60–70 degrees Celsius, 100 mm cubes of control and varied combination proportions were oven-dried for 48 h. After coating its longitudinal surfaces with epoxy paint, the sample was stored in a CO₂ container with a controlled environment. In the chamber, the CO₂ concentration was 5%, the temperature was 27° C, and the relative humidity was 65% [29, 30]. Each specimen was sampled three times at 30, 60, 90, 120, and 180 days for carbonation analysis. For testing, samples were sliced in half lengthwise and sprayed with a phenolphthalein pH indicator. To create the indicator, 1% phenolphthalein was dissolved in 70% ethyl alcohol. This indicator is colorless if the pH is less than 9.2, and purple-red if the pH is more than 9.2. Thus, the average depth and

coefficient of carbonation were calculated for each concrete mix composition.

2.3.9 Acid attack test

According to ASTM C267: 2012, the control mix and a number of other concrete mixes were subjected to acid testing. Before the acid tests, the 100 mm concrete cubes were weighed and tested to determine their compressive strength after 28 days of curing. Each mixture was submerged in fifteen sulfuric acid cubes. The acid solutions were changed every 2 weeks. After 28, 56, and 90 days, the compressive strength of samples was measured and weighed.

2.3.10 Rapid chloride penetration test

A rapid chloride penetration test (RCPT) was conducted on six cells. Methods AASHTO T 277 and ASTM C1202 [31] for chlorination of concrete mixtures. Before this test, cylindrical concrete mixtures of 100 mm in diameter were saturating and dehydrating in a vacuum desiccator. Silicon was placed to the margins of the concrete sample to prevent the escape of chemical solutions. Positive terminal connects to sodium hydroxide, negative terminal to sodium chloride solution. Electrodes made of stainless steel provided the specimens with 60 V dc. Every 30 min, the 6-h current was measured in coulombs. Using total charge, the chloride penetration resistance of concrete mixtures was calculated.

2.4 Morphology and mineralogy

The whole concrete matrix was subjected to SEM, EDS, XRD, TGA/DTG, and FTIR microanalysis. After the mechanical test, a tiny sample was obtained for microanalysis from the region of the fracture. The material was crushed and sieved using a 90- μ m IS sieve. To prevent hydration, acetone was administered immediately. Microanalysis needed 48 h of 60 °C oven-drying.

2.4.1 Scanning electron microscopy (SEM)

After 28 days of hydration, Nova-Nano FE-SEM 450 micrographs characterised concrete mixtures. These SEM images investigated CSH, CH, aggregated NS particles, AFm phase, ITZ, Ettringite, pores, and micro spaces. CSH, CH, agglomerated NS particles, AFm phase, ITZ, Ettringite, pores, and micro voids were analysed in 5000 \times SEM images containing varied NS and MD percentages.

2.4.2 Energy dispersive x-ray analysis (EDX)

To identify the chemical composition of each specimen, a qualitative EDS analysis using line-scan and elemental mapping scan methods (for Si, Ca, O, S, Al, and Fe) on

a Nova Nano FE-SEM 450 (FEI) with an EDAX detector was matched to the SEM image.

2.4.3 X-ray diffraction (XRD)

In this investigation, copper radiation (CuK α) was employed as the X-ray source for the XRD apparatus at 1.54 nm and 40 kV/40 mA. Throughout the experiment, scanning was performed at 2 $^\circ$ /min with a step width of 0.02 $^\circ$ and an angle range of 3 $^\circ$ –90 $^\circ$. Panalytical X-ray PRO reflectometer was used for XRD analysis.

2.4.4 Thermogravimetric analysis

Derivative Thermogravimetry (TG)/(DTG) was used to evaluate the temperature-induced change in sample weight. TGA reports concrete mix pozzolanic component hydration products. During heating, dehydration, degradation, and oxidation of hydration products induce concrete mixture weight variations. Using a Shimadzu-60H TG/DTG device, 25–30 mg of concrete mix sample was heated to 900 °C at a rate of 10 °C per minute.

2.4.5 FTIR spectroscopy

FT-IR spectroscopy evaluated structural changes in specimens (Bruker ALPHA spectrophotometer). The specimens were mixed with KBr for FT-IR analysis in the total attenuated reflection mode between 500 and 4000 cm $^{-1}$.

3 Results and discussion

3.1 Compressive strength

In Fig. 4, the compressive strengths of C-97, C-98, and C-99 were greater than those of the control mix at all ages of curing. C-100 is the weakest while C-98 is the strongest. NS replacement at higher concentrations enhanced the compressive strength of young adults at 1, 3, and 7 days. After 14, 28, 56, and 90 days of curing,

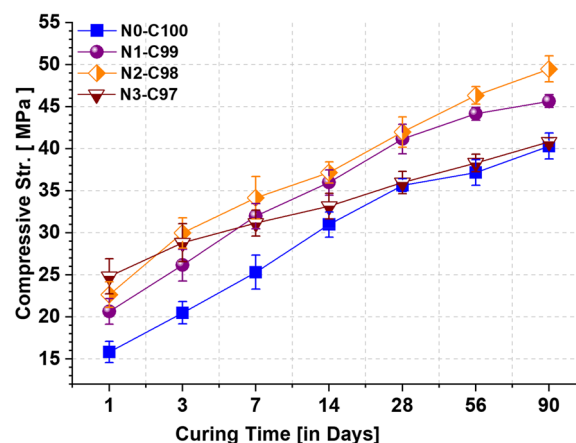


Fig. 4 Compressive strength development with varying substitution of NS (1, 2, 3%)

the rise in compressive strength slowed. Thus, the majority of the NS hydration response occurs during the first week after curing. NS encourages Portlandite $\text{Ca}(\text{OH})_2$ consumption during the first 1–7 days of cure, when high hydration rates are achieved [32]. After curing, hydration products cover the unhydrated cement particle and fill the pores [33]. The use of 3% NS may reduce the increase in compressive strength. The hydration procedure leached extra NS when the particle size of the NS was greater than that of the released lime. The greater surface area of NS draws water, hence inhibiting cement hydration and C-S-H gel formation. This phase utilises NS as a nanofiller, not as a hydration agent. Despite pozzolanic processes, the filling effect improves strength in later phases. Thus, increasing NS in the mixture reduces the amount of water available for hydration [34]. Strength is increased by NS-accelerated secondary nucleation of CSH gel and cement particle hydration. NS particles provide a greater surface area for portlandite $\text{Ca}(\text{OH})_2$ reactivity during secondary nucleation, hence accelerating gelation and enhancing compressive strength. Secondary nucleation boosts concrete strength in the dense C-S-H gel microstructure. When NS is high, uniformity demands a substantial amount of SP. Numerous bubbles in the mixture may reduce its compressive strength. To reinforce the mixture, solidify it longer and more thoroughly. The nanofiller effect and pozzolanic reaction reduce the crystal diameters of calcium hydroxide, hence improving the ITZ [35]. NS interacts more distorted and elongated Ca atoms and decreases their concentration in the concrete matrix [36], hence accelerating C3S degradation and cement hydration (Fig. 4).

3.2 Flexural strength

As shown in Fig. 5, NS and OPC cements impact the flexural strength of binary mix concrete. In terms of flexural strength, C-97, C-98, and C-99 surpassed the reference blend. As shown in Fig. 5, the flexural strength of C-98 and C-99 improved the greatest and decreased the least after curing. Three and seven days after hydration, blends containing NS exhibited greater flexural strength than the control blend. Due to high NS hydration, additional portlandite $\text{Ca}(\text{OH})_2$ was used in the early curing days (ages 1–7). Hydration products encapsulate and cover the unhydrated cement particle's pores, preventing water from entering. This is the reason why strength enhancements over 2% NS replacement have been eliminated. NS fills up the ITZ's minute fissures. As seen in Fig. 5, the flexural strength of NS (3% concrete samples) increased during early curing but decreased with age. A high NS component in a concrete mixture causes excessive self-desiccation and cracking, which may be mitigated to some extent by adjusting the SP dose. NS lowers void

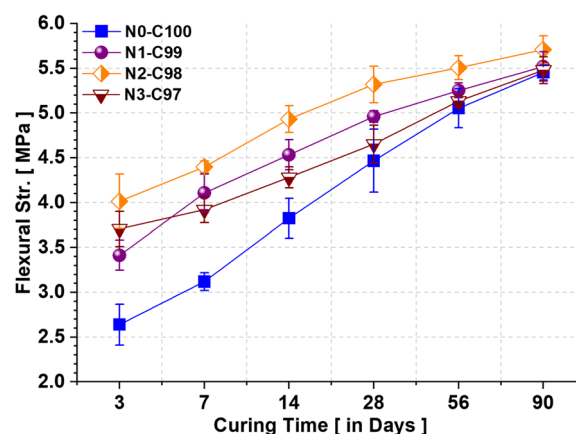


Fig. 5 Flexural strength development with varying substitution of NS (1, 2, 3%)

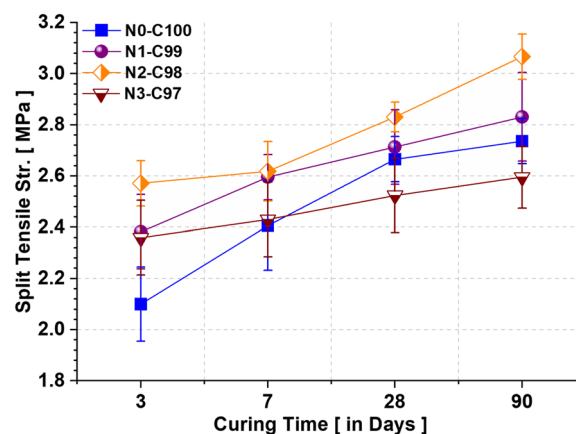


Fig. 6 Split tensile strength development with varying substitution of NS (1, 2, 3%)

pore size in concrete without altering volume. Strong aggregation propensity of NS impacts the freshness and hardness of the concrete mixture. Inefficient NS dispersion while mixing diminishes the strength.

3.3 Split tensile strength

The Split Tensile Strength test (STS) is an essential method used to evaluate various aspects of concrete structures, including shear design, crack propagation, and the effectiveness of reinforcing bar anchorage. The experimental design of our investigation is illustrated in Fig. 6. It is worth mentioning that C-98 had the greatest STS (sulphate resistance) values following both 28 and 90 days of the curing process, beating the reference mix by 11% and 8% correspondingly. In addition, it can be observed from Fig. 6 that both C-98 and C-99 exhibited greater STS values in comparison to the conventional mix. The observed improvement in Short-Term Strength

(STS) can be ascribed to the substitution of cement with nano-silica (NS), resulting in enhancements in both pozzolanic activity and specific surface area. Consequently, this phenomenon promoted the generation of a higher quantity of calcium-silicate-hydrate (C-S-H) gel and a more compact microstructure, thereby leading to a substantial improvement in initial strength.

Nevertheless, it is worth mentioning that when NS was employed as a replacement for cement in mixes with concentrations surpassing 2%, a reduction in split tensile strength was found. This phenomenon can be elucidated by the observation that, during the process of hydration, the leaching of silica from nano-silica particles exceeds that of free lime. The leaching of excessive silica leads to a decrease in split tensile strength in mixtures containing NS concentrations exceeding 2%. This is due to the transition of NS particles from actively participating in the hydration process to primarily acting as fillers.

However, it is worth noting that the inclusion of nano-silica (NS) in concrete significantly enhances both friction and split tensile strength. This is primarily attributed to the increased contact area and enhanced interlocking mechanisms within the dense concrete matrix. The aforementioned phenomenon is also intensified through the interplay between the cement paste and the aggregate at the boundary where they meet, commonly referred to as the Interfacial Transition Zone (ITZ). The inclusion of nanosilica (NS) in the interfacial transition zone (ITZ) demonstrates a notable homogenization effect, resulting in a discernible enhancement in split tensile strength, as evidenced by the obtained outcomes.

In brief, the results of the study are consistent with current scholarly investigations, indicating that the substitution of cement with NS can considerably augment split tensile strength, particularly when NS is incorporated within ideal concentration thresholds. The enhancement in mechanical performance of the concrete mixture can be attributed to the interplay of various elements, including pozzolanic activity, microstructure densification, and optimised interactions within the interfacial transition zone (ITZ). These aspects collectively contribute to the observed increase.

3.4 Static modulus of elasticity

The static modulus of elasticity (SMOE) test on hardened concrete after 28 and 90 days of hydration is shown in Fig. 7. C-97 lowered SOME by 2%, whereas C-98 raised it by 11% and 7.5% relative to the standard blend. C-98 and C-99 have a higher SMOE than the standard mixture. NS concentrations up to 2% improve matrix density, hardness, and SMOE. Agglomeration of NS particles reduces SMOE and creates voids that weaken the matrix. The observed alterations may potentially be ascribed to the

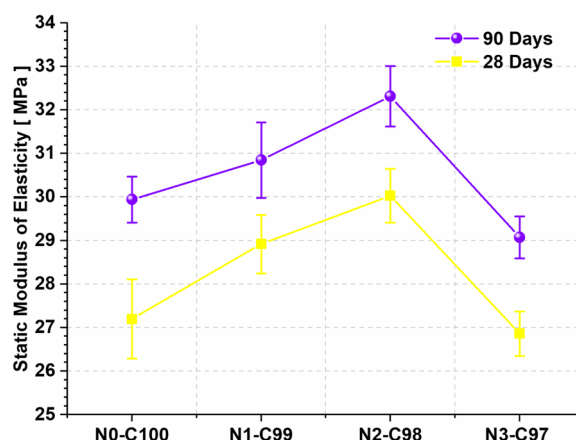


Fig. 7 Static modulus of elasticity development with varying substitution of NS (1, 2, 3%)

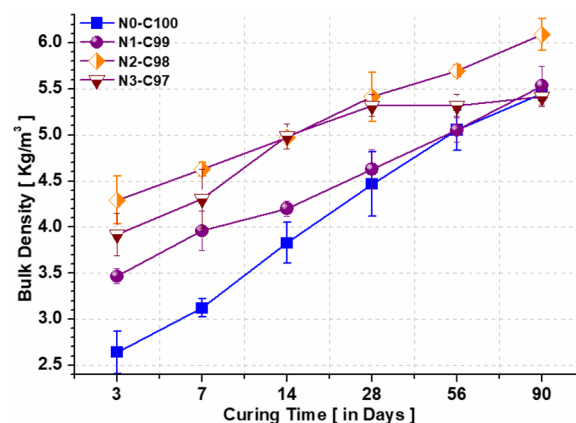


Fig. 8 Bulk density of concrete mixes

interactions occurring between the nanoparticles of the nanosilica (NS) and the cementitious matrix. The compatibility between NS and the matrix can be influenced by various specific features, including particle size, surface area, and chemical composition. These factors can contribute to a localised accelerating effect.

3.5 Bulk density test

The data shown in Fig. 8 illustrates the fluctuations in bulk densities among the concrete mixtures under investigation at various curing time intervals. Significantly, the concrete mixtures that incorporated nano-silica demonstrated elevated bulk densities in comparison to the control mixture. Specifically, concrete mixture C98 had a noteworthy maximum bulk density of 6.1 kg/m³. The observed augmentation in bulk density can be attributed to the incorporation of 2% nano-silica. The enhanced bulk density of concrete can be attributed to the capacity of nano-silica to occupy voids within the concrete

matrix, so effectively filling cavities. Furthermore, the use of nano-silica as a catalyst in cementitious processes assumes a crucial function in facilitating the production of hydration products and serving as a central point for their creation, finally resulting in enhanced bulk density, as elaborated in the study cited as reference [37].

A thorough analysis of the scanning electron microscope (SEM) micrographs presented in Fig. 8 reveals the significant impact of nano-silica on the densification of concrete specimens, as compared to the control mixture. The compactness of the material is a result of the accelerated pozzolanic process promoted by nano-silica. This process lowers the occurrence of voids, leading to an increase in bulk density. It is noteworthy that, as time progresses, there is a tendency for the bulk density of both the control mix and the other concrete mixtures to converge. The observed disparity in bulk density was significant, exhibiting a 64% deviation following a 3-day curing period, which then decreased to 12.9% over a span of 90 days. The observed phenomena can be ascribed to the expedited hydration process triggered by the pozzolanic effect of nano-silica in the initial phases of the curing process. As the duration of the curing process advances, there is a notable increase in density, indicating the ongoing formation and growth of hydration products.

The observed rise in bulk density in concrete mixtures including nano-silica can be attributed to various inter-related mechanisms, such as cavity filling, catalytic promotion of hydration product formation, and quicker pozzolanic processes. The aforementioned mechanisms play a collective role in enhancing the compactness and density of the concrete matrix, particularly during the initial stages of the curing process. This phenomenon lays the groundwork for the observable convergence in density as the duration of curing increases.

3.6 Water absorption test

Figure 9 illustrates the % change in weight as a representation of the water absorption characteristics after subjecting the samples to a 24-h immersion in water, as well as the control combination. Interestingly, the inclusion of nano-silica powder results in a decrease in water absorption. As an example, the incorporation of 1% nano-silica leads to a reduction in water absorption from 3.45% to 1.9%. The aforementioned reduction is also intensified when greater amounts of nano-silica are present. It is worth noting that the incorporation of 2% nano-silica in concrete results in the lowest level of water absorption. On the other hand, the control combination exhibits a decrease in water absorption, dropping from 3.45% to 1.82%. Nevertheless, it is important to highlight that the inclusion of nano-silica beyond 2% results in a reversal of

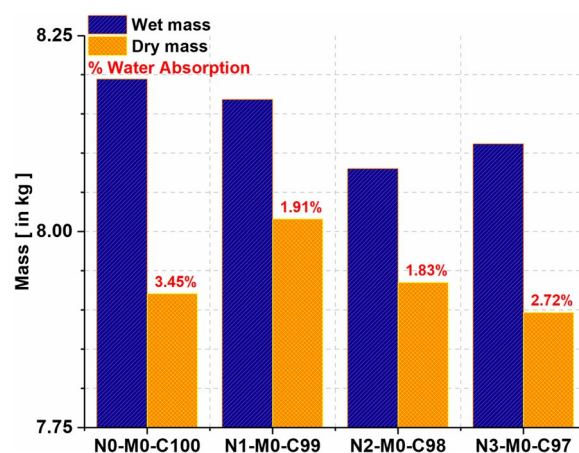


Fig. 9 Mass and Water absorption of concrete mixes

this pattern, leading to an augmentation in water absorption within the concrete mixtures.

The observed phenomena can be ascribed to the distinct influence of nano-silica concentration on the pore structure inside the cement matrix. When the concentration of nano-silica reaches a specific threshold, it has been observed to improve the pore structure of the cement matrix, resulting in a reduction in water absorption. The incorporation of nano-silica powder plays a crucial role in the formation of agglomerates, which in turn contribute to the introduction of porosity within the cement matrix. When the porosity structure is optimised, it functions as an effective barrier to prevent water absorption, hence reducing the permeability of the concrete.

3.7 Din permeability test

The permeability of concrete mixtures is notably influenced by the infiltration of water, as illustrated in Fig. 10. Significantly, the observed pattern in permeability has a strong correlation with the water absorption characteristics. In comparison to the control mixture, the incorporation of nano-silica in isolation results in a significant decrease in permeability. Nano-silica at concentrations of 1% and 2% elicits significant reductions in permeability, amounting to 28% and 50% respectively. The decrease in permeability is most noticeable in the concrete mixture with 2% nano-silica, as seen by a permeability measurement of 6 mm, in comparison to the 14 mm observed in the control mixture.

Remarkably, in accordance with the water absorption experiment, the incorporation of nano-silica over the threshold of 2% tends to reintroduce heightened permeability. The observed modifications can be ascribed to the complex behaviour of silica nanoparticles within

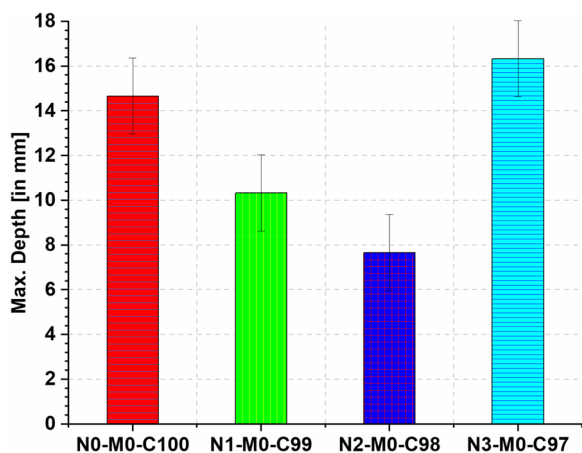


Fig. 10 Depth of water penetration

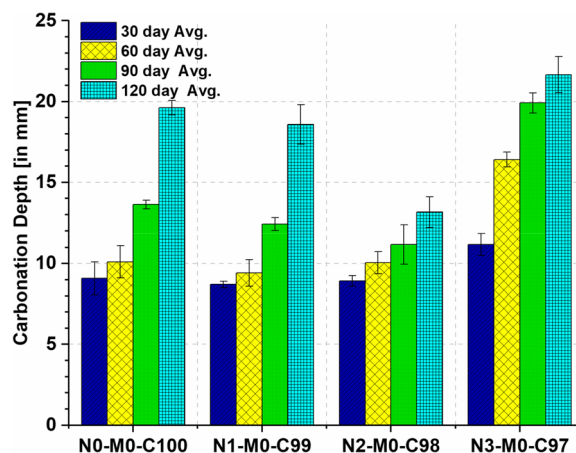


Fig. 11 Carbonation depth of concrete mixes after 30, 60, 90 and 120 days of curing

the concrete matrix. The nanoparticles have a significant impact in impeding the presence of voids, gaps, and capillary pores that are inherent to the matrix. The nanoparticles effectively close these minuscule apertures, hence lowering the dimensions and number of channels via which water infiltration can occur. The combination of pore-blocking and clogging mechanisms results in a notable decrease in the permeability of the concrete mixtures.

In brief, the regulation of permeability through water infiltration exhibits a strong resemblance to the patterns found in the water absorption test. The use of nano-silica, specifically at a specific concentration, enhances the concrete’s ability to resist water infiltration by utilising nanoparticles to efficiently block potential paths for water within the matrix.

3.8 Carbonation test

Carbonation reduces the alkalinity of the pore solution, which may cause concrete degradation. After 30, 60, 90, and 120 days, carbonation penetration depth is measured (Fig. 11). The carbonation depth of the control mixture was 9 mm after 30 days, 10 mm after 14 days, and 20 mm after 120 days. Compared to the control combination, Nano silica powder diminishes the depth of carbonation. The carbonation of samples with 3% Nano silica was more robust. The C98 mix had a minimum value of 13 mm after 120 days, 33% less than the control mix. The first 30 days of the carbonation test revealed no significant differences between concrete mixes with and without Nano silica. As CO₂ exposure rises, the carbonation levels of various compounds change. Carbonation is a process of slow diffusion that improves with time. Calcium carbonate from hydration products precipitates as calcite during carbonation. As the carbonation depth of

C98 decreases, calcite production decreases. With 2% Nano silica, changes in pore structure, densification, and hydration products may diminish carbonation depth.

3.9 Acid attack test

Due to their alkalinity, concrete mixtures are acid-prone. Figure 12. All concrete mixtures with varying constituents vary in density and compressive strength. With Nano silica, concrete mixtures are less prone to acidity. Increased Nano silica powder concentrations make concrete mixtures more resistant to acid, lowering weight change and compressive strength compared to the control mix. Compared to the control mix, the concrete mix containing 2% Nano silica had an 11% weight change and 32% compressive strength change after 90 days of acid curing. The acid resistance of concrete mixes with Nano silica concentrations over 2% is

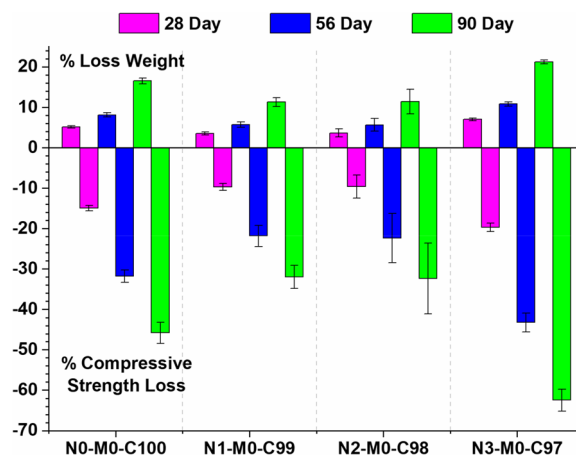


Fig. 12 Change in weight and compressive strength of concrete mixes after exposure to acid attack

diminished. The acid degrades the cement gel binder in the matrix of the concrete, altering its density and strength. From calcium hydroxide, it commonly yields calcium sulphate. Calcium sulphate and calcium aluminates are responsible for the formation of secondary ettringite. The separation of secondary ettringite into silica gel by physical forces. Ions of chloride stimulate calcium hydroxide leaching. In every manner, these ions influence the C-SH layer. Chemical absorption takes place on the outer layer, between layers, or with C-S-H linked to the matrix. Following acid, sulphide, and chloride exposure, decalcification, porous C-S-H, and calcium hydroxide leaching degrade concrete mixture [38]. In two ways, silica nanoparticles provide acid resistance to concrete mixtures. Small particles of varied sizes and morphologies compress concrete by reducing the porosity. Permeability of acidic solutions through the matrix diminishes. Hydration products such as C-S-H gel structures prevent the breakdown of calcium hydroxide and concrete mix. It is resistant to pH.

3.10 Rapid chloride penetration test

After 28 days of curing, all concrete mixtures were RCPT-tested. Figure 13 displays all mixing outcomes coulombically. ASTM C1202-10 guidelines govern data interpretation. Figure 13 depicts RCPT experiments revealing that all concrete mixtures had moderate chloride permeabilities, with charges flowing between 1000 and 2000 coulombs. The C98 and C99 concrete mixtures have a passing charge value that is less than 1000, indicating very low chloride permeability. In comparison to the control combination, the Nano pore-filling silica and pozzolanic actions lower chloride permeability in all samples. NS components boost concrete’s pore structure and density. Thus, replacing cement with nano-silica increases the chloride resistance capacity of concrete and lowers the amount of free chloride ions in the pore system. Since unbound chloride ions promote corrosion of steel reinforcement, eliminating them would increase the durability of concrete. Due to the fact that 3% nano-silica causes agglomeration and big pores, chloride ions may infiltrate concrete mixes more deeply, hence increasing RCPT values.

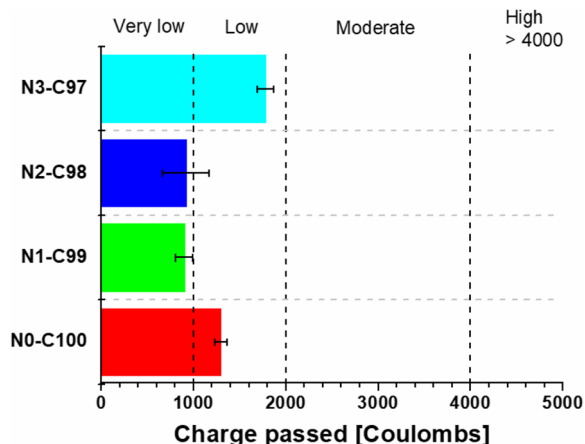


Fig. 13 Rapid Chloride Permeability (Coulombs)

3.11 Cost analysis

The cost of the concrete was determined by multiplying the number of constituents in the concrete mix design by their respective rates. The cost of the concrete mix design was then determined. Fifty kilograms bag of cement is estimated to cost Rs. 360 (based on current market values), while the 1 kg of nano silica is priced at Rs. 1200. The cost estimate does not include labour; it just accounts for materials. Table 3 describes all the calculations of the cost of the materials and concrete for NS0-C100 and NS2-C98 mix. When compared to OPC concrete, concrete incorporated with Nano silica is expensive and but it lowers the usage of cement which may reduce the immersion of carbon dioxide. On comparing the overall performance of Nano silica concrete is much better than ordinary concrete.

Table 3 Cost analysis of NS0-C100 and NS2-C98 mix

Constituent	Cost (in Rupees) ^a	NS0-C100		NS2-C98	
		Quantity (kg/m ³)	Estimated Cost (in Rupees)	Quantity (kg/m ³)	Estimated Cost (in Rupees)
Cement	360/ bag	395	2844	351.55	2531
Nano Silica	1200/kg	-	-	3.95	4740
Fine Aggregate	1400/m ³	676.3	556	676.3	556
Coarse Aggregate	2400/m ³	1204.6	1021	1204.6	1021
Total Cost			4421		8848

^a As per the prevailing market rate

4 Morphology and mineralogy

4.1 SEM analysis

Mechanical test results are validated by qualitative microanalysis. Although microanalysis only provides qualitative data, it can shed light on the mechanical and durability test results. As shown in Fig. 14, the microstructure of the ITZ of concrete containing NS revealed a thick and homogeneous space between the bulk paste and aggregate surface. The ITZ microstructure and surrounding area did not contain any portlandite (CH) crystals of significant size. The ITZ and bulk paste lack distinct borders. The additional C-S-H gel formed by the chemical reaction of NS with CH during hydration is seen in Fig. 14a and c. When NS was replaced, this gel filled the crystal voids in the concrete matrix. The figures demonstrate this. SEM photos show a minute CH crystal particle embedded in the concrete matrix [36]. The NS pozzolanic reaction consumes CH and produces more CSH gel. Denser matrix lowers CH crystal

size. In concrete mixes with a larger cement-NS substitution, micropores were discovered. These micropores may weaken the material. The ITZ microstructure of the control mixture reveals an irregular CSH gel structure, an unevenly porous surface, large portlandite (CH) crystals, and needle-like Aft crystals. Less voids were found in NS integrated concrete than in the control mix. These voids were caused by water-filled regions near the aggregate surface. ITZs of samples containing NS had a denser microstructure and fewer micro fractures, particularly C98, which had a greater influence on porosity reduction and strength gain than the control mix.

4.2 EDS analysis

In addition to the morphological study utilising SEM images, a qualitative EDS analysis was performed using a line-scan and elemental mapping scan technique (for Si, Ca, O, S, AL, Mg, and Fe) to determine the chemical composition of the concrete specimen.

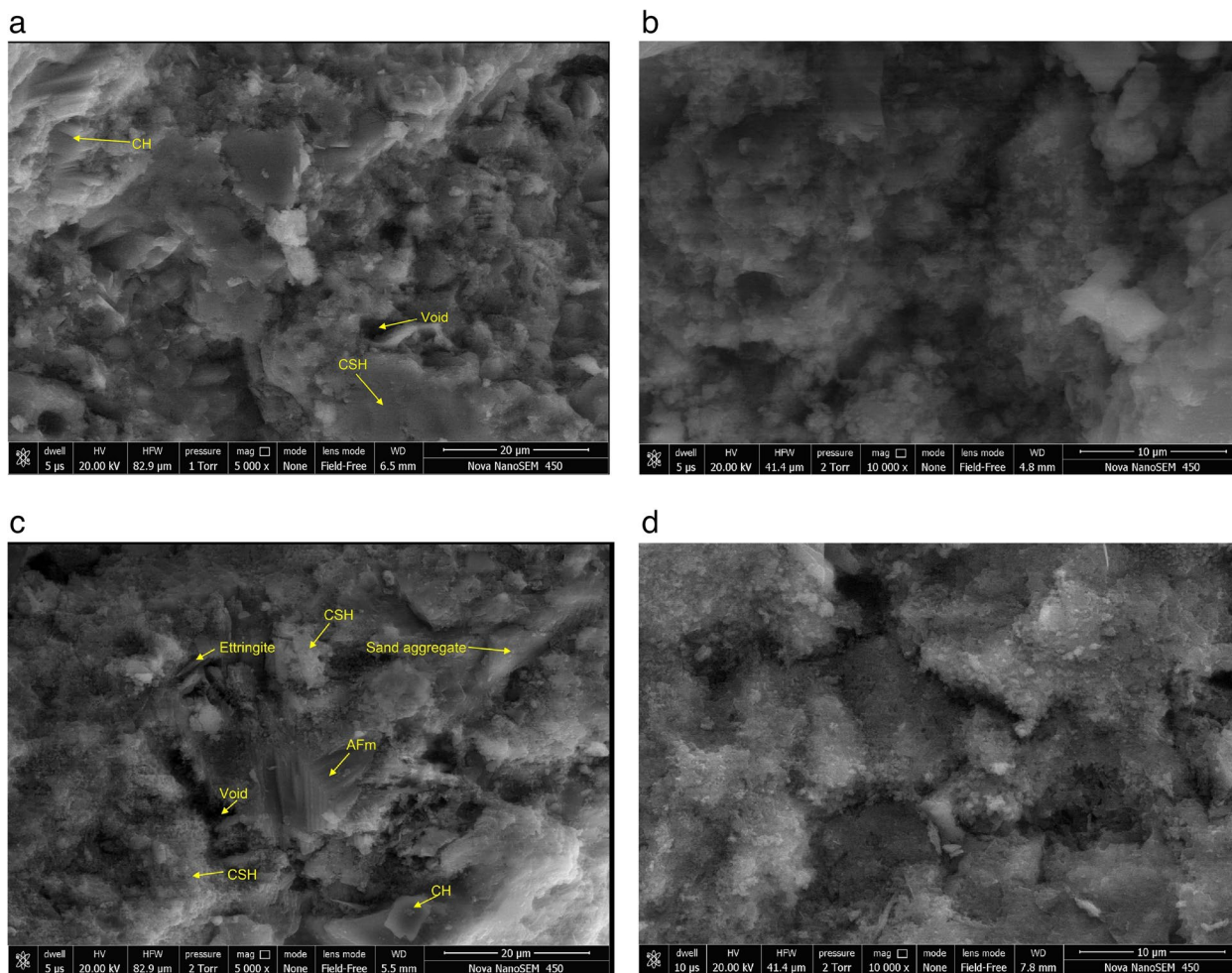


Fig. 14 a SEM Image of C-100. b SEM Image of NS1-C-98. c SEM Image of NS2-C-98. d SEM Image of NS3-C-99

For this examination, the morphological investigation employed SEM images. The relative weight percent and atomic weight percent ratios for Ca/Si, Ca/Al, and Si/Al concrete compositions are shown in Table 4. The mixture has more Si than Al, indicating that the quartz particles will have a more difficulty in dissolving during hydration. As seen in Table 3, NS amounts altered the Ca/Al and Si/Al ratios. The EDX spectrum shown in Fig. 15 revealed adequate amounts of iron and silica. Guaranteed to improve in strength. Increased Ca/Si ratios weaken materials' mechanical properties.

4.3 XRD analysis

Figure 16 displays XRD spectra of concrete mixtures including NS. After 28 days of hydration, the XRD spectra were analysed to identify the different mineralogical phases. XRD patterns were dominated by portlandite (CH), calcite (C), and calcium-silicate compounds (C2S and C3S) as shown in Fig. 16. As a result of the hydration of C3S, crystalline C2S and C3S peaks were found. Since C3S was adequately hydrated. Mechanical characteristics imply that strength has increased. XRD spectra of samples containing 2% NS revealed reduced calcium hydroxide precipitation compared to the control mixture. This demonstrates that NS consumes more calcium hydroxide (CH) and generates more C-S-H gel in the system [39], hence enhancing the mechanical qualities of the concrete mixture. The XRD experiment demonstrated that 2% NS addition used more CH than NS replacement at 3%. Therefore, NS at 2% is more efficient. The cement composition of the concrete may also be to blame. Figure 16 shows the C-S-H peak at 28° in the XRD pattern (c). C-SH reached its peak after 28 days of hydration, confirming the mechanical tests. N.S. 2 percent had a greater C-S-H peak intensity. The concrete samples included unhydrated cement minerals such as ettringite, alite, belite, aluminate, and ferrite, as illustrated in Fig. 16a, c (Ali 2021). As shown in Fig. 16 quartz peak intensity rises with NS replacement rate, which supports the mechanical strength improvement.

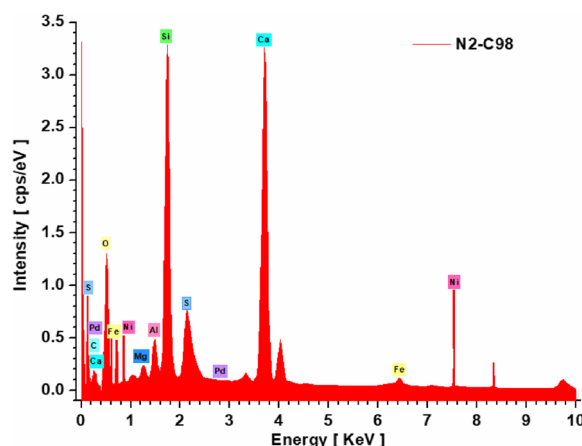


Fig. 15 EDS analysis of C-98

4.4 TGA/DTG analysis

TGA and DTG curves may demonstrate the stability of a mix of fire-resistant concrete at high temperatures. Figure 17 shows the TG and DTG values for selected samples of the current compositions. When heated, all samples respond identically. Three temperature ranges are shown by the TG curves: 30–450 degrees Celsius, 450–700 degrees Celsius, and 700–800 degrees Celsius. As the temperature increases, the first two portions lose weight gradually, but the third section loses weight rapidly. For example, the weight loss for first two portion of N0-C100, N1-C99, N2-C98 and N3-C97 was 7.1%, 5.2%, 8%, and 9.5%, respectively. Whereas for last portion i.e. 700–800 °C, the weight loss was 2.4%, 0.8%, 2.5%, and 1%, respectively. The causes of the first region's weight loss are multifaceted. Typically, three mechanisms cause it. Adsorbed water evaporates up to 150 °C, but beyond that, chemically linked water of hydration products and dehydration of C-S-H and ettringite induce weight loss up to 450 °C. Calcium hydroxide dehydration causes region two's weight loss. The molecule of hydrated calcium carbonate decarboxylates between 700 and 800 degrees Celsius, resulting in a fast change in weight. The change in weight of this area indicates CO₂ outflow during decarbonation. DTG curves exhibit equal three-peak alterations.

Table 4 Relative weight% and atomic% ratio for Ca/Si, Ca/Al and Si/Al

Mix	Weight %			Atomic %		
	Ca/Si	Ca/Al	Si/Al	Ca/Si	Ca/Al	Si/Al
NS0-C100	3.05	10.65	3.49	2.14	7.16	3.35
NS1-C99	1.74	11.52	6.60	1.22	7.77	6.36
NS2-C98	2.41	16.27	6.75	1.69	10.98	6.50
NS3-C97	2.85	13.52	4.75	2.00	9.09	4.55

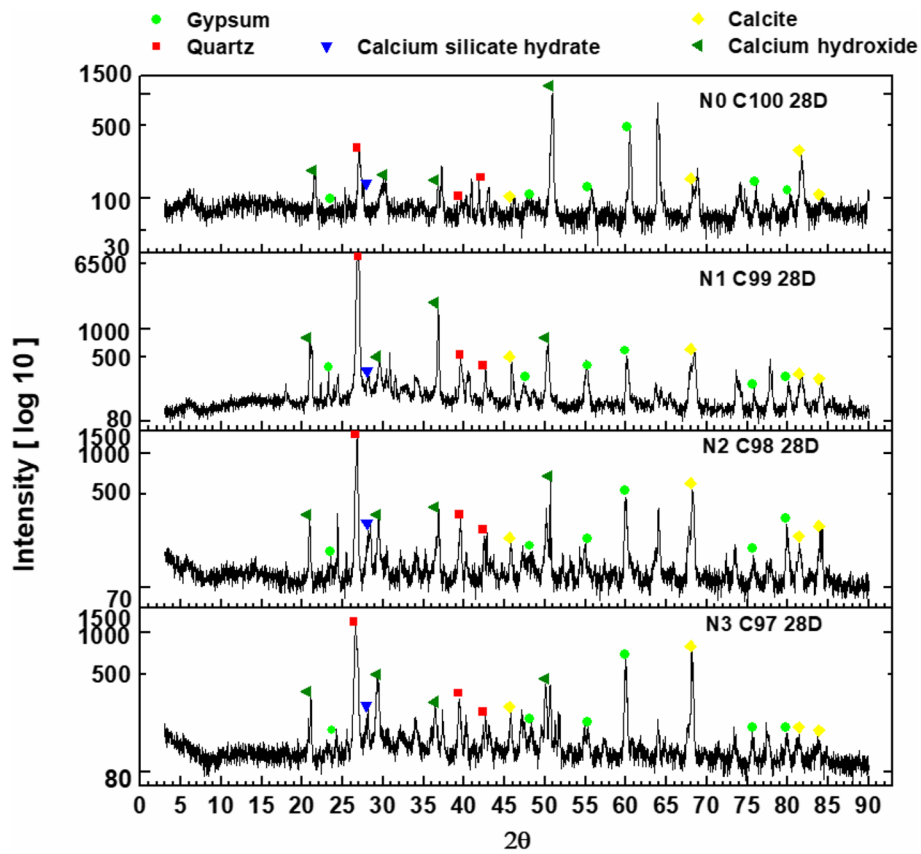


Fig. 16 XRD spectrum of C-100, C-97, C-98 and C-99 after 28 days curing period

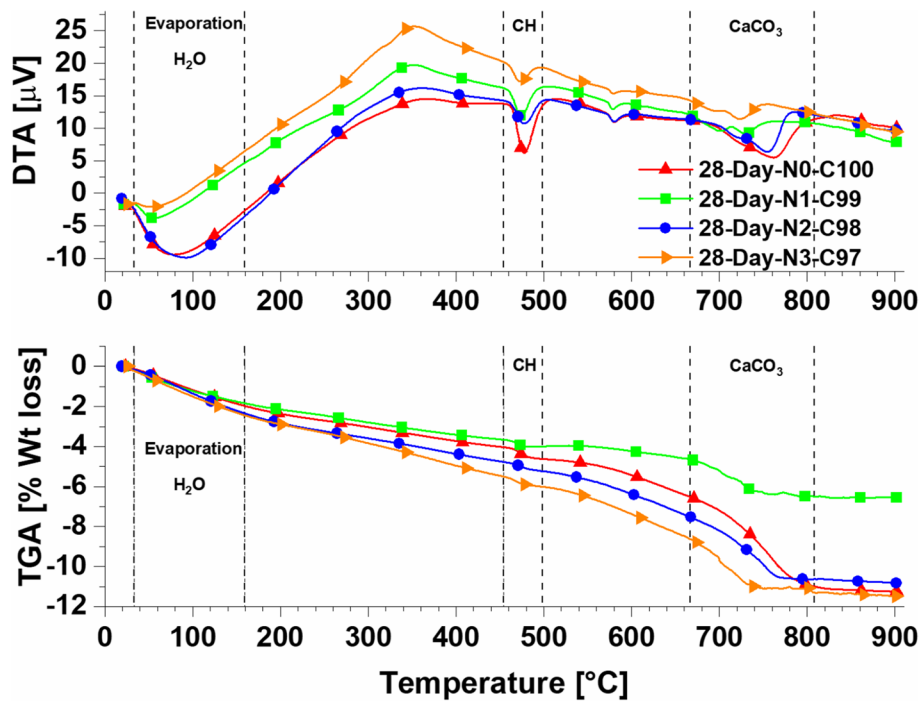


Fig. 17 DTG/TGA curves after 28 days of curing

At 80 degrees Celsius, water evaporates, and at 480 degrees Celsius, C-H and ettringite dehydrate. CaCO₃ decarboxylation creates the third peak at 740 degrees Celsius. According to TGA/DTG curves, concrete mixtures disintegrate beyond 500 °C. The DTG curve (Fig. 17) demonstrates that substituting nano-silica for cement lowers weight loss and stabilises the mixture. All concrete compositions lose volume when cooled. At higher temperatures, nano-silica lowers calcium carbonate concentration and weight loss. As previously stated, increased nanosilica concentrations result in agglomeration, an increase in pore size, a high carbonate content, and significant weight loss.

4.5 FTIR spectroscopy

Si-O asymmetric stretching bonds at 1000 cm⁻¹ produce hydrocarbons such as C-S-H. (Fig. 18). IR spectra have three primary regions. With a wavelength of 850–1200 cm⁻¹, the first zone is extended. Due to stretching band asymmetries, the broad and weak bonds in the second zone have a frequency of 750–800 cm⁻¹. The bending of Si-O-Si bonds makes the third zone 500 cm⁻¹ in width. All samples of concrete exhibit the majority of bands, including 1636 cm⁻¹ and 3400–3650 cm⁻¹. These bands are created by the bending and vibrations of the H-O-H bond. These bands are caused by C3S and C2S hydration products absorbed

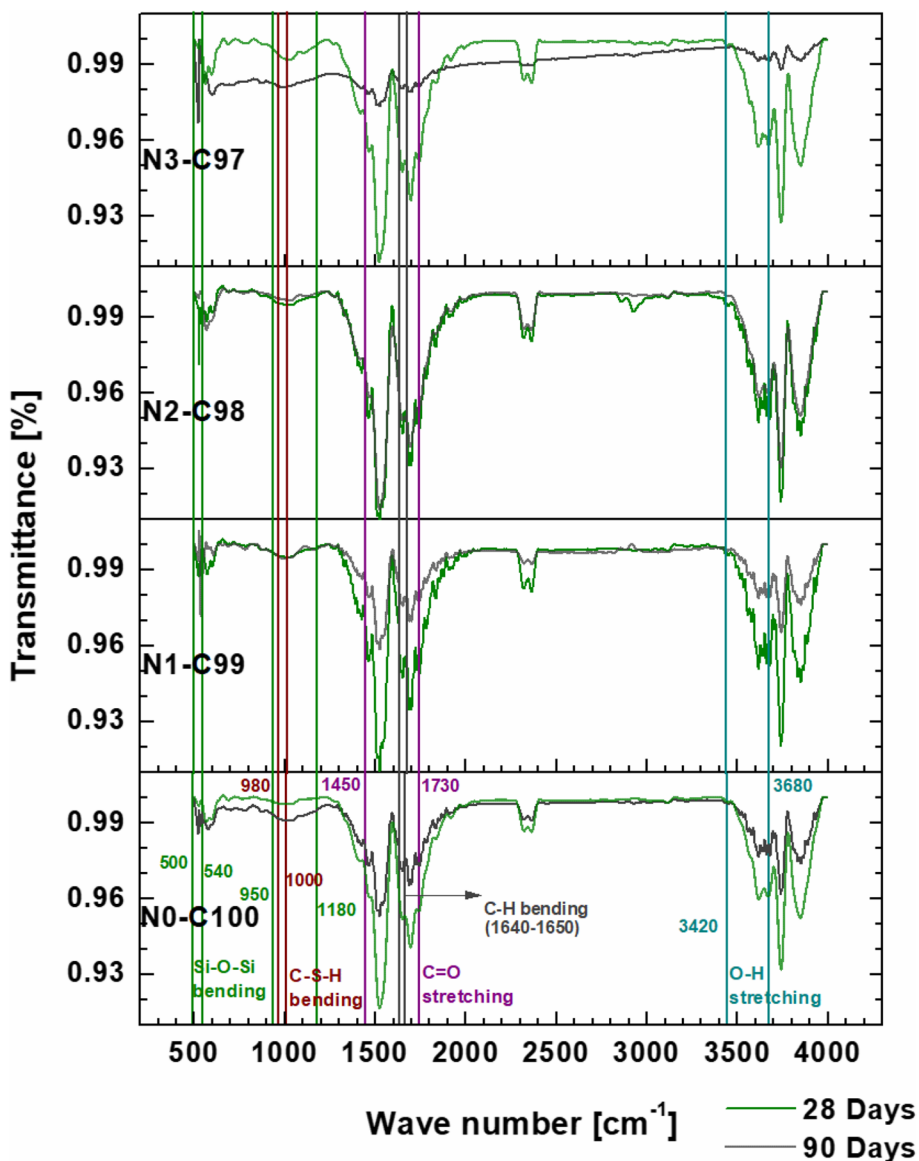


Fig. 18 FTIR spectra of concrete mixes with nano-silica replacement with cement

by concrete mixtures. As curing time and free water diminish, a complex C-S-H gel develops, resulting in a drop in band intensity. After 90 days, these bands are less severe than after 28 days. These bands are diminished more by nano silica samples than by the control concrete mixture. Nano silica specimens exhibit a considerable range of banding.

5 Conclusion

In this work, the mechanical strength, durability properties and microstructure of nano-modified concrete with varying NS replacement ratios were investigated. It was discovered that the addition of NS considerably increased the concrete's mechanical strength when compared to the reference mix. This rapid increase in the early day strength demonstrates the usefulness of NS-modified concrete in construction projects needing rapid strength growth. After 90 days, NS-modified concrete showed less carbonation depth, demonstrating an improved resistance to carbonation. Additionally, the NS-containing concrete samples shown exceptional resistance to sulfuric acid, highlighting the material's potential for use in harsh chemical conditions. NS-modified concrete indicated compact aggregate packing, a denser overall microstructure, and fewer voids. The calcium-silicate-hydrate (C-S-H) and calcium hydroxide (CH) consumption rates in the NS-modified concrete were lower, which may have contributed to the concrete's strength and durability.

Acknowledgements

The authors are thankful to the Central Analytical Facilities (CAF) and Manipal University Jaipur for providing the facilities of mineralogical and morphological testing. The authors also acknowledge the support provided by the Civil Engineering Department, Manipal University Jaipur.

Authors' contributions

All authors contributed to the study conception and design. Material preparation, data collection and analysis were performed by Vikram Kashyap and Gaurav Sancheti. The first draft of the manuscript was written by Jitendra Singh Yadav and all authors commented on previous versions of the manuscript. All authors read and approved the final manuscript.

Funding

The authors gratefully acknowledge the funding provided by Manipal University Jaipur under Seed Grant scheme No EF/2017-18/QE04-14.

Availability of data and materials

Data sharing not applicable to this article as no datasets are associated with this manuscript.

Declarations

Competing interests

The authors have no relevant financial or non-financial interests to disclose.

Received: 30 June 2023 Revised: 30 October 2023 Accepted: 8 November 2023

Published online: 05 December 2023

References

- Folagbade SO, Newlands MD (2014) Suitability of cement combinations for carbonation resistance of structural concrete. *J Eng Des Technol* 12:523–539. <https://doi.org/10.1108/JEDT-08-2012-0033>
- Li PP, Brouwers HJH, Chen W, Yu Q (2020) Optimization and characterization of high-volume limestone powder in sustainable ultra-high performance concrete. *Constr Build Mater* 242:118112. <https://doi.org/10.1016/j.conbuildmat.2020.118112>
- Shaban WM, Elbaz K, Amin M, Ashour AG (2022) A new systematic firefly algorithm for forecasting the durability of reinforced recycled aggregate concrete. *Front Struct Civ Eng* 16(3):329–346
- Mena J, González M, Remesar JC, Lopez M (2020) Developing a very high-strength low-CO₂ cementitious matrix based on a multi-binder approach for structural lightweight aggregate concrete. *Constr Build Mater* 234:117830. <https://doi.org/10.1016/j.conbuildmat.2019.117830>
- Shaban WM, Elbaz K, Yang J, Thomas BS, Shen X, Li L et al (2021) Effect of pozzolan slurries on recycled aggregate concrete: mechanical and durability performance. *Constr Build Mater* 276:121940
- Norhasri MSM, Hamidah MS, Fadzil AM (2019) Inclusion of nano metaclay as additive in ultra high performance concrete (UHPC). *Constr Build Mater* 201:590–598. <https://doi.org/10.1016/j.conbuildmat.2019.01.006>
- Li H, Xiao HG, Yuan J, Ou J (2004) Microstructure of cement mortar with nano-particles. *Compos Part B Eng* 35:185–189. [https://doi.org/10.1016/S1359-8368\(03\)00052-0](https://doi.org/10.1016/S1359-8368(03)00052-0)
- Zhang M, Islam J, Peethamparan S (2012) Cement & concrete composites use of nano-silica to increase early strength and reduce setting time of concretes with high volumes of slag. *Cem Concr Compos* 34:650–662. <https://doi.org/10.1016/j.cemconcomp.2012.02.005>
- Palla R, Karade SR, Mishra G et al (2017) High strength sustainable concrete using silica nanoparticles. *Constr Build Mater* 138:285–295. <https://doi.org/10.1016/j.conbuildmat.2017.01.129>
- Tsardaka EC, Stefanidou M (2019) Application of an alternative way for silica fume dispersion in cement pastes without ultrasonication. *Cem Concr Res* 115:59–69. <https://doi.org/10.1016/j.cemconres.2018.10.002>
- Singh M, Srivastava A, Bhunia D (2019) Long term strength and durability parameters of hardened concrete on partially replacing cement by dried waste marble powder slurry. *Constr Build Mater* 198:553–569. <https://doi.org/10.1016/j.conbuildmat.2018.12.005>
- Ma B, Wang J, Tan H et al (2019) Utilization of waste marble powder in cement-based materials by incorporating nano silica. *Constr Build Mater* 211:139–149. <https://doi.org/10.1016/j.conbuildmat.2019.03.248>
- Qing Y, Zenan Z, Deyu K, Rongshen C (2007) Influence of nano-SiO₂ addition on properties of hardened cement paste as compared with silica fume. *Constr Build Mater* 21:539–545. <https://doi.org/10.1016/j.conbuildmat.2005.09.001>
- Ashraf M, Iqbal MF, Rauf M, Ashraf MU, Ulhaq A, Muhammad H, Liu QF (2022) Developing a sustainable concrete incorporating bentonite clay and silica fume: mechanical and durability performance. *J Clean Prod* 337:130315
- Gesoglu M, Güneyisi E, Asaad DS, Muhyaddin GF (2016) Properties of low binder ultra-high performance cementitious composites: comparison of nanosilica and microsilica. *Constr Build Mater* 102:706–713. <https://doi.org/10.1016/j.conbuildmat.2015.11.020>
- Liu R, Xiao H, Liu J et al (2019) Improving the microstructure of ITZ and reducing the permeability of concrete with various water/cement ratios using nano-silica. *J Mater Sci* 54:444–456. <https://doi.org/10.1007/s10853-018-2872-5>
- Fallah S, Nematzadeh M (2017) Mechanical properties and durability of high-strength concrete containing macro-polymeric and polypropylene

- fibers with nano-silica and silica fume. *Constr Build Mater* 132:170–187. <https://doi.org/10.1016/j.conbuildmat.2016.11.100>
18. Cheng Y (2019) Experimental study on nano-SiO₂ improving concrete durability of bridge deck pavement in cold regions. 2019.
 19. Shaban WM, Elbaz K, Yang J, Shen SL (2021) A multi-objective optimization algorithm for forecasting the compressive strength of RAC with pozzolanic materials. *J Clean Prod* 327:129355
 20. Mahdikhani M, Bamshad O, Fallah Shirvani M (2018) Mechanical properties and durability of concrete specimens containing nano silica in sulfuric acid rain condition. *Constr Build Mater* 167:929–935. <https://doi.org/10.1016/j.conbuildmat.2018.01.137>
 21. Singh LP, Ali D, Tyagi I et al (2019) Durability studies of nano-engineered fly ash concrete. *Constr Build Mater* 194:205–215. <https://doi.org/10.1016/j.conbuildmat.2018.11.022>
 22. Bureau of Indian Standards (BIS) (1990) BIS: 8112. Indian standard specification 43 grade ordinary Portland cement specification. Bureau of Indian Standards, New Delhi. [Reaffirmed in 2013]. Indian Stand 17
 23. Bureau of Indian Standards (BIS) (1959) BIS: 516, Indian standard methods of tests for strength concrete. Bureau of Indian Standards, New Delhi. [Reaffirmed in 2004]
 24. Bureau of Indian Standards (BIS) (1999) BIS: 5816, Indian standard splitting tensile strength of concrete—method of test. Bureau of Indian Standards, New Delhi. [Reaffirmed in 2004]
 25. American Society for Testing and Materials (2002) ASTM C469–02: Standard test method for static modulus of elasticity and poisson's ratio of concrete in compression. ASTM Standard Book 4:1–5
 26. IS:6441(Part-1) (1972) IS-6441-1-1972 Methods of test for autoclaved cellular concrete products, part 1: determination of unit weight or bulk density and moisture content. Bur Indian Stand, New Delhi
 27. ASTM C642-06 (2008) ASTM C 642 standard test method for density, absorption, and voids in hardened concrete. In: *Standar Test Method Density, Absorption, Voids Hardened Concr.* pp 11–13
 28. G. Deutsches Institut für Normung, Berlin (1991) Determination of permeability of concrete, in: DIN 1048 (Part 5)
 29. Elsalamawy M, Mohamed AR, Kamal EM (2019) The role of relative humidity and cement type on carbonation resistance of concrete. *Alexandria Eng J* 58:1257–1264. <https://doi.org/10.1016/j.aej.2019.10.008>
 30. Chen Q, Zhang H, Ye J et al (2023) Corrosion resistance and compressive strength of cemented soil mixed with nano-silica in simulated seawater environment. *KSCE J Civ Eng* 27:1535–1550. <https://doi.org/10.1007/s12205-023-1240-4>
 31. ASTM C1202 (2012) ASTM C1202 standard test method for electrical indication of concrete's ability to resist chloride ion penetration. *Am Soc Test Mater* 1–8. <https://doi.org/10.1520/C1202-12.2>
 32. Berra M, Carassiti F, Mangialardi T et al (2012) Effects of nanosilica addition on workability and compressive strength of Portland cement pastes. *Constr Build Mater* 35:666–675. <https://doi.org/10.1016/j.conbuildmat.2012.04.132>
 33. Chithra S, Senthil Kumar SRR, Chinnaraju K (2016) The effect of colloidal nano-silica on workability, mechanical and durability properties of high performance concrete with copper slag as partial fine aggregate. *Constr Build Mater* 113:794–804. <https://doi.org/10.1016/j.conbuildmat.2016.03.119>
 34. Bernal J, Reyes E, Massana J et al (2018) Fresh and mechanical behavior of a self-compacting concrete with additions of nano-silica, silica fume and ternary mixtures. *Constr Build Mater* 160:196–210. <https://doi.org/10.1016/j.conbuildmat.2017.11.048>
 35. Ismael R, Silva JV, Carmo RNF et al (2016) Influence of nano-SiO₂ and nano-Al₂O₃ additions on steel-to-concrete bonding. *Constr Build Mater* 125:1080–1092. <https://doi.org/10.1016/j.conbuildmat.2016.08.152>
 36. Sancheti G, Kashyap VS, Yadav JS (2021) Mechanical and microstructural behavior of concrete containing marble and nano silica. *J Eng Des Technol.* <https://doi.org/10.1108/JEDT-08-2021-0413>
 37. Heikal M, Abd El Aleem S, Morsi WM (2013) Characteristics of blended cements containing nano-silica. *HBRC J* 9:243–255. <https://doi.org/10.1016/j.hbrj.2013.09.001>
 38. Gaitero JJ, Campillo I, Guerrero A (2008) Reduction of the calcium leaching rate of cement paste by addition of silica nanoparticles. *Cem Concr Res* 38:1112–1118. <https://doi.org/10.1016/j.cemconres.2008.03.021>
 39. Nazerigivi A, Najigivi A (2019) Study on mechanical properties of ternary blended concrete containing two different sizes of nano-SiO₂. *Compos Part B Eng* 167:20–24. <https://doi.org/10.1016/j.compositesb.2018.11.136>

Publisher's Note

Springer Nature remains neutral with regard to jurisdictional claims in published maps and institutional affiliations.